Stochastic resonance of the visually evoked potential

R. Srebro* and P. Malladi
Department of Ophthalmology and Department of Biomedical Engineering, University of Texas, Southwestern Medical School, 5323 Harry Hines Boulevard, Dallas, Texas 75235
(Received 17 September 1998)

Stochastic resonance refers to the enhancement of a signal by the addition of a small amount of noise and its degradation by a larger amount of noise. It occurs in a variety of physical systems including neuronal systems. However, its demonstration in neuronal systems has so far been limited to single-dimensional systems such as a single mechanoreceptor. We report here the existence of stochastic resonance in the visually evoked potential, a very high-dimensional neuronal system. [S1063-651X(99)51203-8]

PACS number(s): 05.20.−y, 87.10.+e

The term stochastic resonance (SR) was introduced by Benzi *et al.* [1,2]. It refers to the enhancement of signal-to-noise ratio (SNR) by the addition of low intensity noise and the subsequent degradation of SNR by the addition of more noise. A thorough review of SR has recently appeared [3]. Early studies suggest that the term SR is appropriate when a nondetectable signal is made detectable by noise, but here we use the current and broader definition that includes enhancement of an already detectable signal. SR has been observed in several nonlinear systems forced by a weak periodic function including Schmitt Trigger circuits, ring lasers, electron paramagnetic systems as well as in several neuronal systems: crayfish mechanoreceptor [4], human muscle spindle [5] and rat cutaneous mechanoreceptor [6], all single-dimensional neuronal systems. Although SR is possible in multidimensional systems, a clear demonstration of its existence in a large scale neuronal system is wanting. And since natural neuronal systems incorporate internal sources of noise it is possible that such systems are already optimized for SNR. Here we report the existence of SR in the visually evoked potential (VEP) in humans, a mass response reflecting a very large number of cortical cells.

VEP's are due to the leakage of synaptic current through the skull. Large cells oriented orthogonal to the cortical surface, pyramidal cells, appear to be the source (and sink) of the current [7]. The current causes a weak potential field on the scalp (microvolt range). A VEP with a peak-to-peak amplitude of 4 mV requires 10 to 20 cm^2 of cortical surface area to supply sufficient current; this corresponds to approximately 10^8 cortical neurons [8]. Counter phase temporal modulation of the contrast of a spatial grating (contrast reversal) results in a ''steady-state'' VEP. This VEP is nonlinear. It shows harmonic distortion, consisting of multiple even harmonics of the stimulus frequency, and an amplitude versus contrast function that saturates at 30 to 60% contrast. The VEP originates in the visual area of the cortex called visual area 1 (*V*1). This area located in the occipital region at the back of the head receives the entire subcortical input from the lateral geniculate nucleus. In cat and primate, *V*1 contains two major cell types, simple and complex. Multiple simple cells feed forward to a complex cell but only after a threshold nonlinearity. That is the simple cells must first generate all or none nerve impulses to transmit to complex cells. Simple cells are linear up to the generation of nerve impulses [9]. A simple cell can thus be characterized by a linear spatiotemporal receptive field [10]. There are several types of simple cells. Each simple cell has a partner with a spatiotemporal receptive field that is shifted 180° in the temporal phase as well as another partner whose spatiotemporal field is in spatial quadrature. As a result, a contrast reversal grating stimulus produces synaptic currents that, in a population of simple cells, cancel, while the complex cell that is fed by the population of simple cells responds with a modulated synaptic current at twice the frequency of the stimulus. A drifting grating, on the other hand produces only a steady (dc) synaptic current in the complex cell. The steady-state VEP to contrast reversing and drifting gratings has properties similar to those of a complex cell.

We measured the VEP produced by stimuli consisting of a square wave spatial grating plus two-dimensional spatial-temporal noise. The grating was black and white, its spatial frequency was 4 cycles per degree (cycles/deg) and its contrast was 20%. It was counter phase modulated (contrast reversal) at 4 Hz (8 reversals of contrast per second). The noise was binary, consisting of black and white elements each subtending 3.5 min of arc. It was updated at 60 Hz. The spatial frequency spectrum of the noise was flat to 20.4 cycles/deg (3 db point). The temporal frequency spectrum of the noise was flat to 29 Hz (3 db point). Noise contrast was varied from 0 to 50% in steps of 10% (0,10,20,30,40, and 50%). The space average luminance of the stimulus remained constant at all times. The noise and the grating shared the same video screen which was refreshed at 120 Hz, alternating noise and grating at a frequency well above both human perception and the VEP frequency response.

Thirteen subjects, medical and graduate students, viewed the stimuli binocularly from 1 m in a dimly lit room, from which distance the screen was subtended 17.8°. Stimuli were presented in epochs of 15 s. Noise was presented continuously at the same contrast throughout the epoch. The grating was presented for 5 s (20 cycles), commencing at the fifth second of the epoch. An experimental run consisted of 18

*Author to whom correspondence should be addressed. Present address: Dept. of Ophthalmology, University of Texas, Southwestern Medical Center, Dallas, TX 75235-8592. FAX: 214-630-8841. Electronic address: dick@striate.swmed.edu

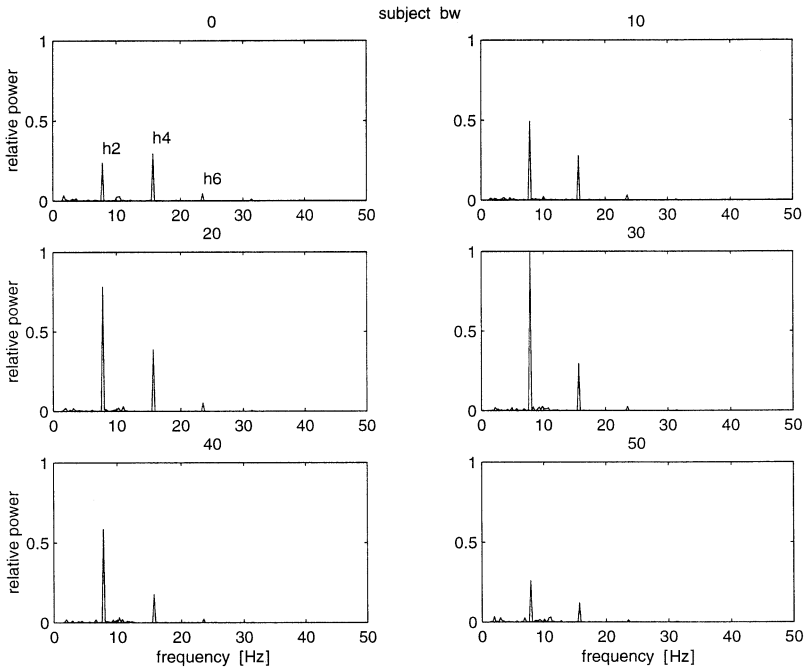

FIG. 1. Power spectra of VEPs for a single subject. Each panel shows the power spectrum in the presence of noise at the noise contrast marked above it.

such epochs and lasted 4.5 min. Noise contrast was randomly selected for each epoch; each experimental run contained three epochs at each noise contrast. Each subject sat for five experimental runs in a single recording session. The subjects were instructed to fixate on a small green dot at the center of the screen that remained constant and were allowed to rest for as long as they wished between runs.

Sixteen gold-cup electrodes were placed on the posterior half of the scalp at approximately 5 cm intervals to cover the scalp from inion to vertex and from mastoid to mastoid with a regular tessellation. The electrode at the vertex served as the reference electrode. The right ear was used as ground. The experiments were carried out according to an IRB approved protocol.

The electroencephalogram (EEG) recorded at each electrode was analog filtered (1 to 100 Hz, 1 pole Butterworth) digitized at 200 Hz and stored on disc along with a logic voltage level indicating the grating phase and with identifying information for each epoch. The EEGs were digitally filtered (1.5 to 56 Hz, 8 pole Butterworth, zero phase shift). The 5 s portion corresponding to the grating presentation was extracted and the first 4 cycles (1 s) of grating stimulation were removed because this segment contained a transient VEP caused by the onset of the grating (not artifact). These data were used to estimate the average VEP and the power spectrum of the VEP. The average VEP was calculated for each cycle of stimulus presentation; 16 cycles were averaged within each data segment and 240 cycles ($16\times3\times5$) were averaged for each subject and noise contrast across all five experimental runs. The average VEP was calculated separately at each electrode. The power spectrum of each data segment was calculated and averaged for each noise contrast across epochs and runs. Because a data segment corresponded exactly to an integer number of stimulus cycles (16), a rectangular window was used and each ''bin'' represented an independent estimate of power. The spectral resolution was 0.25 Hz. EEG noise was estimated by averaging the power over 8 bins (2 Hz) above and 8 bins below a frequency of interest. Evoked power occurred only at even harmonics of the stimulus frequency. The power spectra and noise estimates were calculated separately for each electrode. The electrode with the best signal-to-noise ratio was taken for analysis.

Figure 1 shows VEP power spectra for one subject at the electrode on the scalp overlying *V*1, which was the electrode with the best overall SNR. This location usually produced the largest VEP. Measurable VEP power was present only at even harmonics of the stimulus up to at least the sixth harmonic but most of the VEP power was measured with in the first two even harmonics ($h2$ and $h4$, 8 and 16 Hz, respectively). VEP power was progressively enhanced by noise up to a noise contrast of 30% and then degraded as noise contrast was increased above 30%. Figure 2 shows the same data in more detail. The power of the second harmonic of the VEP was increased 4.2 fold by noise, peaking at 30% noise contrast. The estimated EEG noise was nearly flat across all noise contrasts and the SNR was accordingly increased by noise. The power of the fourth VEP harmonic was also increased 1.3 fold by noise, peaking at 20% noise contrast. Again, EEG noise did not change with noise contrast. The average VEP, Fig. 3, consisted of two nearly identical waves presumably corresponding to each contrast reversal of the stimulus. The amplitude of the average VEP was progressively enhanced by noise by a factor of approximately 1.6 up to noise contrast 30% and diminished as noise contrast was further increased.

Figure 4 shows data similar to that shown in Fig. 2 but for all 13 subjects as an average taken across all subjects. Not all subjects showed results as striking as those presented in Figs. 1–3, but all showed some degree of enhancement of VEP power near 30% noise contrast. Overall, $h2$ power increased by a factor 2.1 while $h4$ power increased by a factor of 1.2 and the estimated EEG noise remained constant as noise contrast increased. The average VEP (not shown but similar to Fig. 3) was also progressively enhanced by noise peaking in

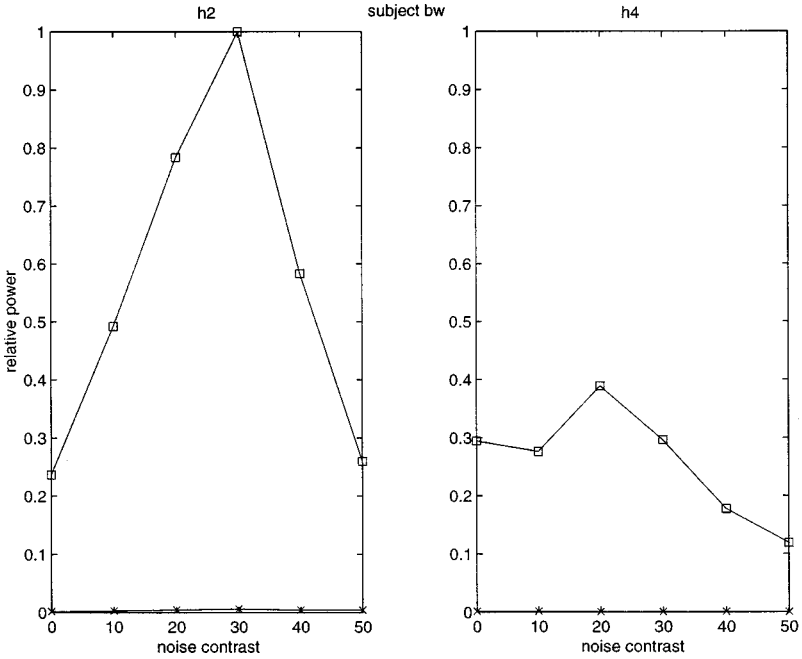

FIG. 2. VEP power as a function of noise contrast for a single subject. Each panel shows the power for a single harmonic of the VEP marked above it (*h*2, second harmonic, 8 Hz; *h*4, fourth harmonic, 16 Hz). Open squares: VEP signal power. Crosses: EEG noise power.

amplitude at a noise contrast of 30%. The increase in VEP amplitude was nearly twofold.

The hallmark of SR, from which it derives its name is a peaked relationship between SNR and noise. Both the average VEP as well as the power of the first two even harmonics exhibit this signature. It was previously reported that some perceptual processes, such as the detection of light touch, exhibit SR [11], but we do not know how many cortical neurons subserve the detection of a weak sensory signal near threshold. The demonstration here that SR occurs in the VEP represents clear evidence that SR can occur in a neuronal system of massive dimension. Also the existence of SR in the VEP shows that this neuronal system is not naturally optimized for internal noise.

There was no evidence that the noise of EEG increased measurably with the contrast of the applied visual noise. We examined the noise only segments of the records as well as the signal plus noise segments and still found no change in EEG noise with visual noise. We also examined a broader range of the spectrum for evidence that the visual noise caused brain activity that was somehow shifted in frequency to higher or lower frequencies, but with the same negative result. The most likely explanation for this failure to find a change in EEG noise with applied visual noise, is that the EEG noise derives from a very large region of the cortex, not just *V*1, regions which may not respond to visual stimulation. That is, the EEG noise is a ''whole brain'' noise but the EEG response to visual noise is specific to the visual cortex and constitutes a small fraction of the whole brain noise.

The existence of SR in the VEP could be the result of the threshold intervening between the linear responses of simple cells and the post-synaptic activity of the complex cells that

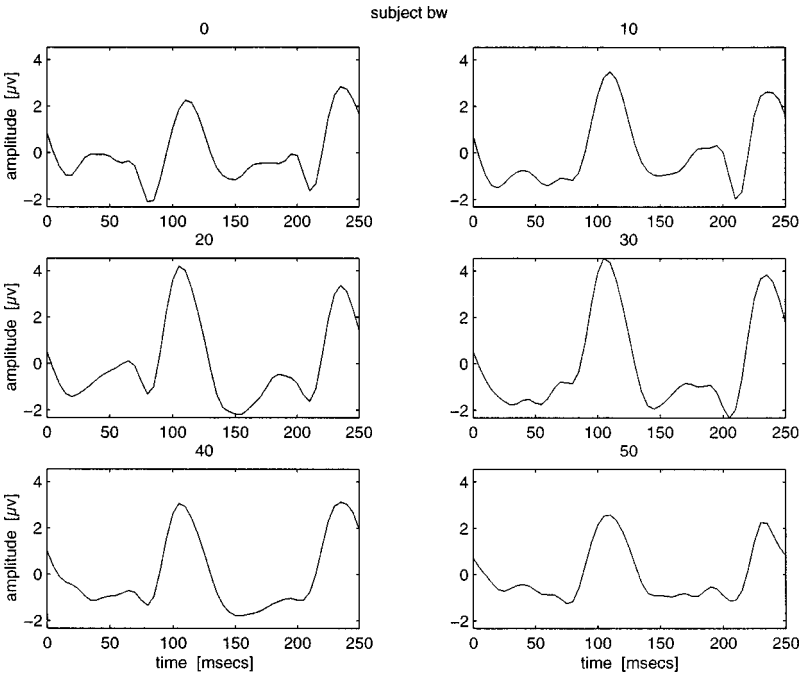

FIG. 3. Average VEP's for a single subject. Each panel shows the average VEP for one cycle of stimulation (two contrast reversals) at the noise contrast marked above it.

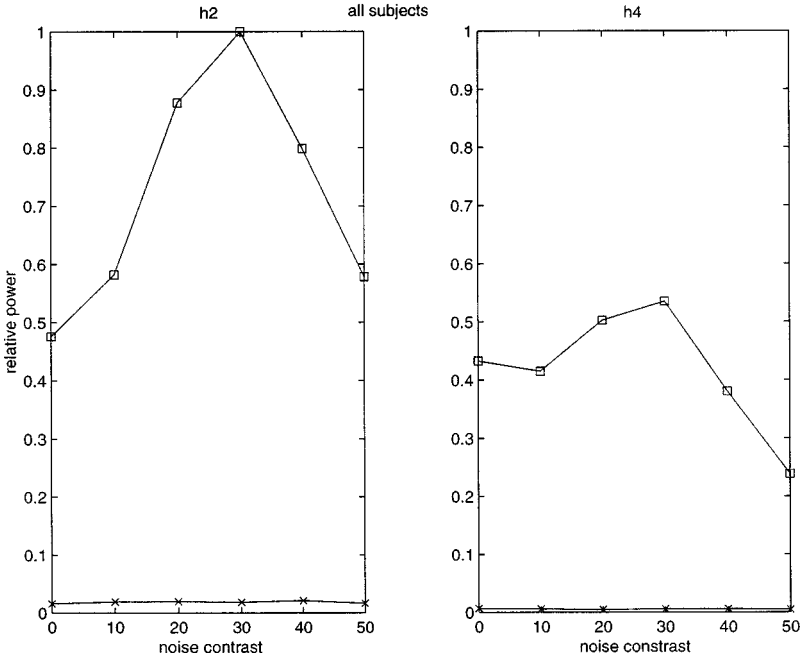

FIG. 4. VEP power as a function of noise contrast for all subjects. Symbols as in Fig. 2.

they drive. We tested this hypothesis by simulating the experiment in a model system. The model consisted of 100 simple cells sharing a single linear spatiotemporal receptive field that spanned approximately one spatial grating cycle. All 100 simple cells spanned five grating cycles with a regular tessellation. Thus each simple cell sampled a different phase of the grating. Test stimuli were simulated by mixing a square wave counter phase modulation of the grating with spatio-temporal noise mimicking that used in the experiment. The linear response of each simple cell was obtained by convolving each test stimulus with the linear spatiotemporal field. The full wave rectified output of each simple cell was operated on by a hard threshold such that impulse functions were generated at 200 Hz as long as the threshold was exceeded. This simulated nerve impulse generation. The simulated nerve impulse rates were always well below saturation. The outputs of all the simple cells were summed and the spectrum was calculated for this sum to estimate the amplitudes of the second and fourth harmonics as a function of noise contrast. The background noise was estimated as in the experimental analysis as well.

Figure 5 shows the results of the simulation. A spatiotem-

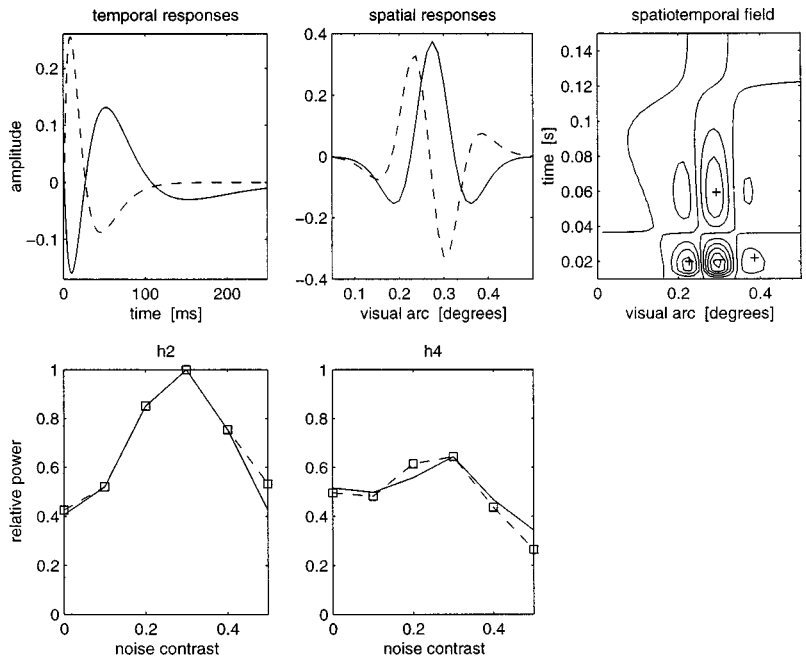

FIG. 5. Simulation of SR experiment. Nerve impulse responses from a population of 100 simple cells were summed and the power spectrum calculated for different visual noise contrasts. See text for details. panel one shows temporal response functions and panel two spatial response functions that resulted from fitting the SR data. Panel three shows the ''equivalent'' spatio-temporal field that best fit the SR data built from the temporal and spatial response functions in panels one and two. The last two panels show the quality of the fit of the simulation (continuous curve) to the SR data (dashed curve with boxes).

poral receptive field was constructed using two temporal response functions and two spatial response functions. The temporal response functions were calculated as suggested by Wimbauer *et al.* [12]. There are two classes of temporal response functions called lagged and nonlagged. The nonlagged function is illustrated by the continuous curve in the first panel of Fig. 5. It contains one free parameter to adjust its waveform. The lagged function is illustrated by the dashed curve in that same panel. It has two free parameters to adjust its waveform. The lagged function differs from the nonlagged function in that it has a negative-positive onset. Lagged and nonlagged temporal response functions are characteristic of the temporal responses of cells in the lateral geniculate nucleus and occur in about equal proportions [13]. The spatial response functions were calculated to mimic those observed in simple cells following Adelson and Bergen [14]. The profiles are the differences of Gaussians and are set by a single parameter. The two profiles are the same function but in spatial quadrature. The spatiotemporal field shown in the third panel is the sum of two spatiotemporal fields. The first is the product of the nonlagged temporal response function and the original spatial response function (shown as a continuous line in the second panel). The second is the product of the lagged temporal response function and the spatial quadrature profile (shown as a dashed line in the second panel). Adding these two spatio-temporal fields produces a single spatiotemporal field that is ''nonseparable'' (it cannot be reconstructed as the product of a single time function and a single spatial profile) and is similar to actual spatiotemporal fields observed in simple cells. The last two panels show that the SR seen in the VEP could be accounted for by a single ''equivalent'' spatiotemporal field and a threshold for firing nerve impulses. The equivalent spatiotemporal field is shown in the third panel and was determined by adjusting the five parameters of the model (three temporal parameters, one spatial parameter, and the threshold) to obtain a best least-squared fit using a gradient search (steepest descent) method. The temporal and spatial response functions that resulted from the fit to the data are those actually shown in panels one and two.

Our model, based on observed properties of simple and complex cells in the visual cortex, is somewhat different from and yields different results from a generic summing network model proposed by Collins, Chow, and Imhoff [15]. The generic model consisted of a set of excitable units (*EU*'s, FitzHugh-Nagumo model neurons); each *EU* received the same signal but identically and independently distributed Gaussian noise. SR was observed in the generic model when the number of *EU*'s was small (1–10) but when the number of *EU*'s was large (1000), SNR increased monotonically with noise power reaching a plateau. In our model for the visual cortex, each simple cell *(EU)* receives a signal that is correlated with but not identical to that received by its neighbors because the spatiotemporal fields of the simple cells only partially overlap. The simple cells also receive correlated noise. In this case, SR does not plateau with visual noise contrast but shows the classical signature of SR, optimization of SNR with a particular visual noise contrast.

[1] R. Benzi, A. Sutera, and A. Vulpiani, J. Phys. A **14**, L453 (1981).
[2] R. Benzi, G. Parisi, A. Sutera, and A. Vulpiani, SIAM (Soc. Ind. Appl. Math.) J. Appl. Math. **43**, 565 (1983).
[3] L. Gammaitoni, P. Hanggi, P. Jung, and F. Marchesoni, Rev. Mod. Phys. **70**, 223 (1998).
[4] J. K. Douglass, L. Wilkens, E. Pantazelou, and F. Moss, Nature (London) **365**, 337 (1993).
[5] P. Cordo *et al.* Nature (London) **383**, 769 (1996).
[6] J. J. Collins, T. T. Imhoff, and P. Grigg, J. Neurophysiol. **76**, 642 (1996).
[7] U. Mitzdorf, J. Neurosci. **33**, 33 (1987).
[8] P. L. Nunez, *Electric Fields of the Brain* (Oxford University Press, Oxford, 1981).
[9] B. Jagadeesh, H. S. Wheat and D. Ferster, Science **262**, 1901 (1993).
[10] D. L. Heeger, E. P. Simoncelli, and J. A. Movshon, Proc. Natl. Acad. Sci. USA **93**, 623 (1996).
[11] J. J. Collins, T. Imhoff, and P. Grigg, Nature (London) **383**, 770 (1996).
[12] S. Wimbaurer, O. G. Wenisch, K. D. Miller and J. L. Hemmen, Biol. Cybern. **77**, 453 (1997).
[13] A. B. Saul and A. L. Humphrey, J. Neurophysiol. **64**, 206 (1990).
[14] E. H. Adelson and J. R. Bergen, J. Opt. Soc. Am. A **2**, 284 (1985).
[15] J. J. Collins, C. C. Chow and T. Imhoff, Nature (London) **376**, 236 (1995).